Optics Letters

Bandwidth-enhanced LFM signal generation by period-one dynamics in a directly modulated semiconductor laser

Gengze Wu,[1] Fangzheng Zhang,[1,*] Xiaoyue Yu,[1] Xin Yan,[1] Hao Wang,[1] Yuan Yu,[2] and Shilong Pan[1]

[1]National Key Laboratory of Microwave Photonics, Nanjing University of Aeronautics and Astronautics, Nanjing 210016, China
[2]Wuhan National Laboratory for Optoelectronics, Huazhong University of Science and Technology, Wuhan 430000, China
*zhangfangzheng@nuaa.edu.cn

Received 14 February 2025; revised 29 April 2025; accepted 30 April 2025; posted 1 May 2025; published 21 May 2025

Period-one (P1) laser dynamics provide effective methods for radar signal generation. However, the linearly frequency-modulated (LFM) signal bandwidth generated by P1 dynamics is constrained by the limited variation range of the injection strength. In this Letter, a bandwidth-enhanced LFM signal generation method by P1 dynamics in an optically injected directly modulated semiconductor laser (DM-SL) is proposed. In addition to controlling the injection strength via electro-optical modulation, which is the same as the previous schemes, the bias current of the DM-SL is regulated via direct modulation. By interaction between the carrier effect and temperature effect in the optically injected DM-SL, the P1 oscillation frequency is increased under the same optical injection strength, leading to the generation of LFM signals with enlarged bandwidth. In the experiment, the maximum signal bandwidth reaches 21 GHz (11.7–32.7 GHz), which is enhanced by 11 GHz compared with that generated without bias current regulation. The proposed method is a promising technique for ultra-wideband radar signal generators.

https://doi.org/10.1364/OL.559656

Linearly frequency-modulated (LFM) signals characterized by large bandwidths have found widespread application in radar systems [1]. Traditional LFM signal generators based on direct digital synthesis (DDS) usually have a bandwidth lower than 2 GHz [2], making it challenging to achieve high radar range resolution. To address this problem, numerous photonics-assisted methods have been proposed for broadband LFM signal generation. Among these methods, the utilization of period-one (P1) dynamics in an optically injected semiconductor laser (OISL) system for broadband signal generation has been the subject of extensive investigation. By dynamically controlling the light of a master laser (ML) injected into a slave laser (SL), these OISL systems can generate broadband frequency-modulated signals [3–5], frequency-hopping signals [6], and multi-chirp signals [7]. However, a common problem with the previous approaches is that, when controlling the injection strength using a Mach–Zehnder modulator (MZM), the dynamic range of the injection light is limited by the modulation index of the MZM, and hence the bandwidth of the generated microwave signals is still limited, which makes it challenging to generate LFM signals with a bandwidth greater than 10 GHz. In fact, by appropriately tuning the injection parameters, the tuning range of P1 oscillation frequency f_0 could reach nearly 100 GHz [8]. In a recent report [9], LFM signals with extended bandwidth were generated by dynamically controlling the injection strength and the detuning frequency. In this method, a MZM is employed to control the injection strength, while a dual-parallel MZM is utilized to control the detuning frequency. The results in [9] show that it is possible to extend the LFM signal bandwidth generated by a traditional OISL system, which is highly required in constructing high-resolution radars [10].

In this Letter, we propose and demonstrate a bandwidth-enhanced LFM generator by P1 dynamics in a directly modulated semiconductor laser (DM-SL). Besides controlling the injection strength, the bias current of the DM-SL is adjusted via direct modulation, leading to an increased P1 oscillation frequency under the same optical injection strength. Compared with the traditional method only using injection strength modulation, the bandwidth of the generated LFM signals is increased effectively. The performance of the proposed method is investigated through proof-of-concept experiments. The maximum bandwidth of the generated LFM signals could reach 21 GHz (11.7–32.7 GHz), which is increased by 11 GHz compared with that generated without bias current regulation.

Figure 1 shows the schematic diagram of the proposed LFM signal generator. The light generated by an ML at frequency of f_m passes through an MZM before injected to a DM-SL through an optical circulator (CIR). To maximize the injection efficiency, a polarization controller (PC) is used before the DM-SL to ensure the polarization state of the ML is aligned with that of the DM-SL. When the bias current of DM-SL is set to I_{SL}, its free-running frequency is f_s, and the detuning frequency between the ML and DM-SL is denoted by f_i ($f_i = f_m - f_s$), as indicated by the optical spectrum before injection in Fig. 2(a). After optical injection, by appropriately setting the parameters, P1 dynamics can be excited. This process generates a regenerated optical carrier at the frequency f_m, along with a redshifted sideband f_s', as

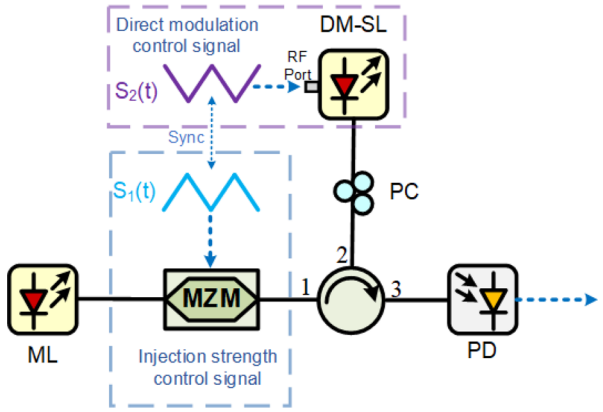

Fig. 1. Schematic diagram of the proposed LFM signal generator.

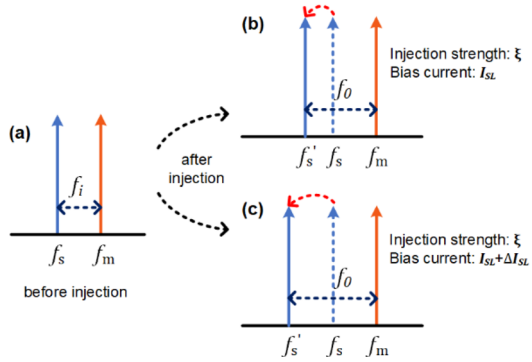

Fig. 2. Schematic of the optical spectrum of (a) free-running ML and DM-SL before injection, (b) P1 laser dynamics, and (c) P1 laser dynamics with increased DM-SL bias current.

indicated by the optical spectrum in Fig. 2(b). The P1 oscillation frequency is represented by f_0 ($f_0 = f_m - f_s'$). After optical-to-electrical conversion, a microwave signal at the frequency of f_0 can be generated. Here, the optical injection strength is defined as ξ ($\xi = \sqrt{(P_{inj}/P_{SL})}$), in which P_{inj} and P_{SL} are the power of injection signal and free-running SL, respectively.

Since the P1 oscillation frequency increases almost linearly as the optical injection strength is enlarged, a microwave LFM signal is generated when a control signal $S_1(t)$ is fed to the input port of the MZM to fast modulate the optical injection strength. In the previous investigations, it is found that, for a proper detuning frequency, the bandwidth of the generated LFM signal can easily reach several gigahertz. However, it is difficult to further enlarge the signal bandwidth, mainly because the variation range of the injection strength is limited. To address this problem and generate ultra-wideband LFM signals, we introduce another control signal $S_2(t)$ to modulate the DM-SL. In this process, when the bias current of the DM-SL is fast varied through direct modulation, the DM-SL is concurrently influenced by the carrier effect [11] and the thermal effect [12]. As the bias current into the semiconductor laser increases, the carrier effect leads to an increase in the carrier density in the active region, which in turn reduces the effective refractive index, ultimately causing a blueshift in the laser wavelength. The thermal effect, on the other hand, causes the temperature in the active region to rise, which leads to an increase in the effective refractive index, resulting in a redshift in the laser emission wavelength. Thanks to the fact that the wavelength shift caused by the thermal effect is more significant (2–3 orders of magnitude larger) [13], a further wavelength redshift is induced on the basis of P1 oscillation, as indicated by the spectrum in Fig. 2(c). Therefore, the instantaneous P1 oscillation frequency of the optically injected DM-SL would be increased under the same optical injection strength, which finally leads to the generation of an LFM signal with effectively enlarged bandwidth.

To verify the feasibility of the proposed LFM signal generation method, experiments are implemented based on the setup in Fig. 1. The ML is a wavelength-tunable laser (CoBriteDX4) of which the wavelength is set to 1549.27 nm, and the power can be adjusted from 10 to 16 dBm. The DM-SL is a commercial 7-pin butterfly-packaged distributed-feedback (DFB) semiconductor laser (Micro Photons, PL-DFB-1550-C-A81-PA-7-BF) with a radio frequency (RF) input port. The direct modulation bandwidth of the DM-SL is 23 GHz, and its threshold is 7 mA. The MZM (Fujitsu, FTM7937EZ) has a bandwidth of ~25 GHz. A low-speed electrical signal generator (ESG, RIGOL DG4062, 500 Msa/s) is used to generate two synchronized control signals ($S_1(t)$, $S_2(t)$). The output signal is converted to electrical domain via a 50 GHz photodetector (Finisar XPDV2120RA). The waveform of the generated LFM signal is analyzed by a real-time oscilloscope (Keysight UXR0254B) working with a sampling rate of 128 GSa/s, and the spectrum is measured by an electrical spectrum analyzer (ESA, Rohde & Schwarz FSWP50). The optical spectrum of the free-running SL and the output from the ML are measured using an optical spectrum analyzer (OSA, Yokogawa AQ6370D) with a resolution of 0.02 nm.

In the experiment, the P1 oscillation frequencies are investigated by manually tuning the output power of the ML and/or the DC-bias current of the DM-SL. First, the bias current of the DM-SL is fixed to be 29.6 mA. The free-running DM-SL emits light at 1549.31 nm with an output power of 5.2 dBm. In this case, the detuning frequency is 5.1 GHz. By adjusting the power of the ML to let the injection strength vary linearly from 0.33 to 0.6, with a step of 0.027, the P1 oscillation frequency is measured by analyzing the frequency of the generated microwave signal, which is found to be changed by 6.7 GHz, i.e., from 14.8 to 21.5 GHz, as shown by the black curve in Fig. 3. Subsequently, as the injection strength changes from 0.33 to 0.6 with a step of 0.027, the corresponding DC-bias current of the DM-SL is adjusted from 29.6 to 39.6 mA with a step of 1 mA. The P1 oscillation frequency is changed from 14.8 to 31.9 GHz, as shown by the red curve in Fig. 3. It is clear that, for the same injection strength, the P1 oscillation frequency is obviously increased when the bias current of the DM-SL increases. The total P1 oscillation frequency variation is also enlarged to be 17.1 GHz. This result proves the potential of increasing the LFM signal bandwidth by changing the bias current of the DM-SL.

Next, LFM signal generation by P1 dynamics of optically injected DM-SL is demonstrated. To this end, the bias current of the DM-SL is set to 32 mA. The corresponding free-running wavelength is 1549.32 nm, and the output power is 5.8 dBm. The profile of control signal $S_1(t)$ generated by the ESG is shown in Fig. 4 (a), where $S_1(t)$ has a period of 10 μs and an amplitude of ~3.75 V. Given that the transfer function of the MZM is a cosine function, $S_1(t)$ is designed as a quasi-triangular profile to compensate for the nonlinearity [3]. When the direct modulation control signal $S_2(t)$ is not applied, the temporal waveform of the generated LFM signal is recorded by the oscilloscope, as shown in Fig. 4(b). Figure 4(c) shows the time–frequency diagram

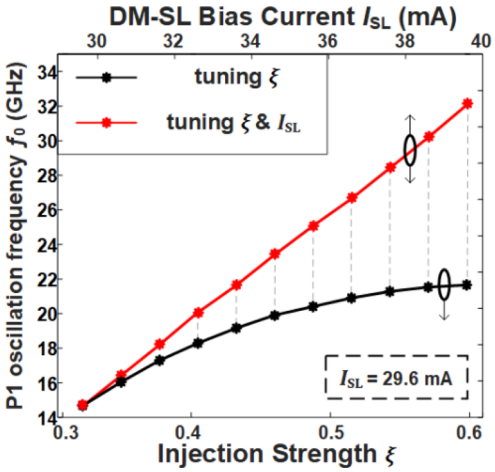

Fig. 3. P1 oscillation frequency varies with tuning ξ, while the DC-bias current I_{SL} is fixed at 29.6 mA (black curve) and varies with tuning ξ and I_{SL} (red curve).

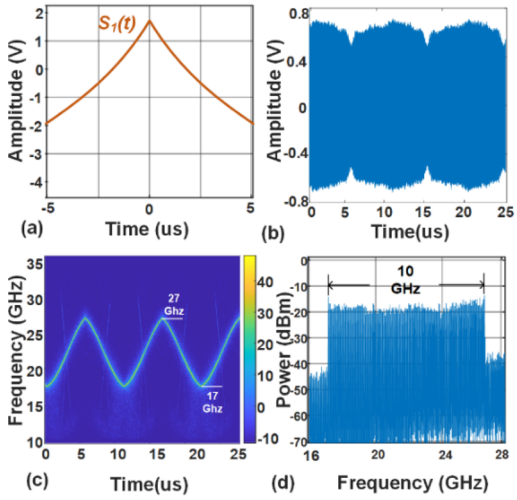

Fig. 4. (a) Control signal $S_1(t)$, (b) measured temporal waveform, (c) calculated instantaneous time–frequency diagram, and (d) measured spectrum (RBW: 100 kHz) of the generated LFM signal with a bandwidth of 10 GHz (17–27 GHz).

obtained by performing short-time fast Fourier transformation (STFFT) to the temporal waveform. As shown in Figs. 4(c) and 4(d), the instantaneous frequency changes from 17 to 27 GHz, indicating that the generated LFM signal has a bandwidth of 10 GHz. Figure 4(d) shows the measured electrical spectrum (resolution bandwidth (RBW): 100 kHz) of the obtained LFM signal. To check the spectrum property after optical injection, the optical spectrum of the signal from the DM-SL is measured and shown in Fig. 5 (black curve), in which a regenerated optical carrier, a spectrally broadened redshifted sideband, and four-wave mixing (FWM) idlers are obviously observed. Here, the bandwidth of the generated LFM signal is determined by the spectral width of the redshifted sideband.

Furthermore, to increase the signal bandwidth, the direct modulation control signal $S_2(t)$ is introduced. The profiles of both $S_1(t)$ and $S_2(t)$ are given in Fig. 6(a). The offset voltage (V_{DC}), amplitude, and period of $S_2(t)$ are −1.17 V, 1.5 V, and 10 μs,

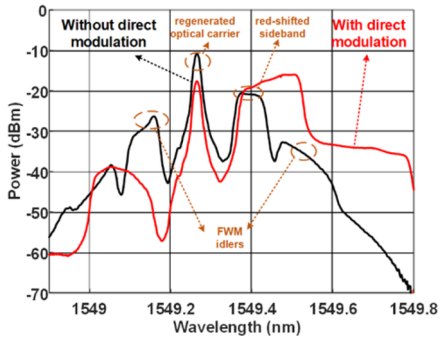

Fig. 5. Measured optical spectrum of P1 laser dynamics without direct modulation (black curve) and with direct modulation (red curve).

respectively. The two control signals are generated by two channels of the ESG, which works in the in-phase operating mode to ensure the two control signals are synchronous. It is worth noting that, due to the circuit design of the butterfly-packaged DFB DM-SL, a decrease in the voltage of the control signal $S_2(t)$ results in an increase in the bias current of the laser. Thus, to match the influence of the injection strength and bias current on the DM-SL within one period, a phase difference of π needs to be introduced between $S_1(t)$ and $S_2(t)$. The temporal waveform and calculated time–frequency diagram are given in Figs. 6(b) and 6(c), respectively. Figure 6(d) shows the measured electrical spectrum (resolution bandwidth (RBW): 100 kHz) of the obtained LFM signal. As shown in Figs. 6(c) and 6(d), the instantaneous frequency changes from 15 to 29 GHz, indicating that the generated LFM signal has a bandwidth of 14 GHz. Therefore, the signal bandwidth is enhanced by 4 GHz compared to the signal generated without direct modulation. It should be noted that, because of the existence of FWM idlers, weak harmonic components are observed in the electrical spectrum in Fig. 6(c). In practical applications, the influences of harmonics can be alleviated by using proper optical or electrical filters in the system.

The previous demonstration proves the capability of bandwidth enhancement by applying direct modulation to the DM-SL. With the proposed direct modulation method, the bandwidth of the generated LFM signals can be further enlarged by adjusting the amplitude of $S_2(t)$. To show this property, the profile of $S_1(t)$ is kept unchanged, as shown in Fig. 4(a). The offset voltage of $S_2(t)$ is fixed at −1.17 V, while the amplitude of $S_2(t)$ is increased gradually. Figures 7(a) and 7(b) show the calculated time–frequency diagrams of the generated LFM signals when the amplitude of $S_2(t)$ is ~3.6 V and ~5 V, respectively. The corresponding signal bandwidths are enlarged to be 16.5 GHz (13.5–30 GHz) and 19 GHz (12.5–31.5 GHz). Figure 7(c) shows the time–frequency diagram of the generated LFM signal when the amplitude of $S_2(t)$ is further increased to ~6.125 V. In Fig. 7(c), the signal bandwidth is found to be 21 GHz (11.7–32.7 GHz), which is enhanced by 11 GHz compared to that generated without direct modulation. This bandwidth enhancement can also be observed in the optical spectrum measured at the output of the DM-SL, as shown by the red curve in Fig. 5. The spectral width of the redshifted sideband is significantly enlarged compared to that of the redshifted sideband generated without direct modulation. For the generated LFM signal in Fig. 7(c), the time–bandwidth product (TBWP)

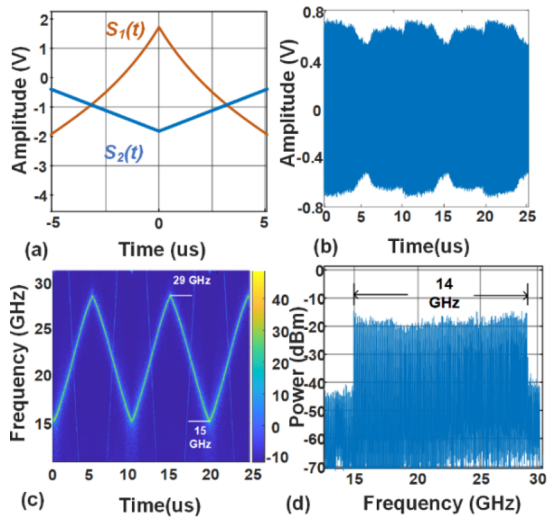

Fig. 6. (a) Control signal $S_1(t)$ and $S_2(t)$, (b) measured temporal waveform, (c) calculated instantaneous time–frequency diagram, and (d) measured spectrum (RBW: 100 kHz) of the generated LFM signal with a bandwidth of 14 GHz (15–29 GHz).

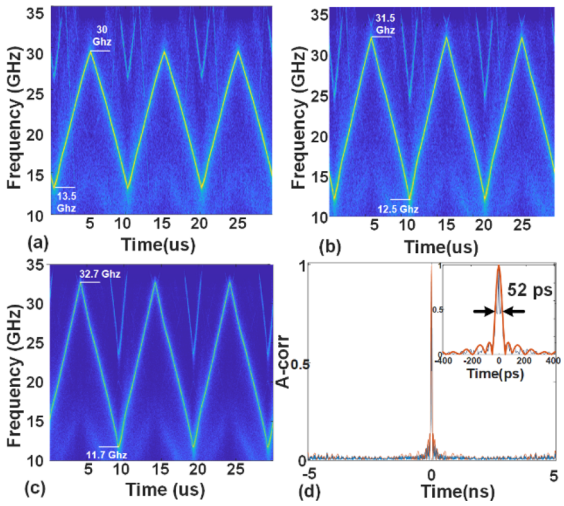

Fig. 7. Calculated time–frequency diagrams of the generated LFM signals with bandwidths of (a) 16.5 GHz (13.5–30 GHz), (b) 19 GHz (12.5–31.5 GHz), (c) 21 GHz (11.7–32.7 GHz) and (d) autocorrelation result for the generated LFM signal with a bandwidth of 21 GHz and a zoom-in-view of the autocorrelation peak.

reaches 21,000. To evaluate the pulse compression capability using this LFM signal, autocorrelation of the recorded waveform is calculated with the result shown in Fig. 7(d). A detailed analysis of the zoomed-in view reveals a full width at half maximum (FWHM) of approximately 52 ps for the autocorrelation peak, corresponding to a pulse compression ratio (PCR) of 19231 and a range resolution of 7.8 mm. In the experiment, because of the limited bandwidth of the oscilloscope and PD, the generation of higher frequency LFM signals is not demonstrated. However, considering that a typical P1 oscillation frequency can reach 100 GHz by choosing a proper detuning frequency, the proposed method is capable of generating LFM signals in high-frequency bands with much larger signal bandwidth. Besides, to improve the signal quality of the generated LFM signals, an optoelectronic feedback mechanism realizing Fourier-domain mode-locking can be introduced to the system to suppress the instantaneous frequency phase noise [14].

In conclusion, a bandwidth-enhanced LFM generator realized by P1 dynamics in a DM-SL is proposed and demonstrated. By combining the injection strength modulation with direct modulation of the DM-SL, the bandwidth of the generated LFM signals is increased effectively compared with the traditional method only using injection strength modulation. In the experiment, the generated triangular LFM signal with a bandwidth of 21 GHz is realized, which achieves 11 GHz bandwidth enhancement compared to the signal generated without direct modulation. The proposed method shows significant potential for ultra-wideband radar signal generation.

Funding. National Natural Science Foundation of China (61871214); Natural Science Foundation of Jiangsu Province (BK20221479); Open Project Program of Wuhan National Laboratory for Optoelectronics (2022WNLOKF002); Open Fund of IPOC (BUPT).

Disclosures. The authors declare no conflicts of interest.

Data availability. Data underlying the results presented in this Letter are not publicly available at this time but may be obtained from the authors upon reasonable request.

REFERENCES

1. A. Meta, P. Hoogeboom, and L. P. Ligthart, IEEE Trans. Geosci. Remote Sens. **45**, 3519 (2007).
2. A. Cavarra, G. Papotto, A. Parisi, *et al.*, Electronics **10**, 531 (2021).
3. P. Zhou, F. Zhang, and S. Pan, J. Lightwave Technol. **36**, 3927 (2018).
4. G. Sun, Y. Zhou, Y. He, *et al.*, IEEE Trans. Microwave Theory Techn. **72**, 6996 (2024).
5. G. Sun, F. Zhang, X. Yu, *et al.*, IEEE Trans. Radar Syst. **2**, 690 (2024).
6. X. Yu, F. Zhang, X. Li, *et al.*, Opt. Lett. **49**, 4266 (2024).
7. B. Nakarmi, B. Y. Song, I. A. Ukaegbu, *et al.*, J. Lightwave Technol. **42**, 184 (2024).
8. A. Hurtado, I. D. Henning, M. J. Adams, *et al.*, IEEE Photonics J. **5**, 5900107 (2013).
9. P. Zhou, J. Zhu, R. Zhang, *et al.*, Opt. Lett. **47**, 3864 (2022).
10. S. Kueppers, T. Jaeschke, N. Pohl, *et al.*, IEEE Sens. Lett. **6**, 3500204 (2022).
11. B. R. Bennett, R. A. Soref, and J. A. Del Alamo, IEEE J. Quantum Electron. **26**, 113 (1990).
12. S. L. Woodward, U. Koren, B. I. Miller, *et al.*, IEEE Photonics Technol. Lett. **4**, 1330 (1992).
13. M. Kuznetsov, IEEE J. Quantum Electron. **24**, 1837 (1988).
14. X. Lin, G. Xia, Z. Shang, *et al.*, Opt. Express **27**, 1217 (2019).